Articles

Specific Binding of α-Macroglobulin to Complement-Type Repeat CR4 of the Low-Density Lipoprotein Receptor-Related Protein†

Olav M. Andersen,‡ Peter A. Christensen,‡ Lisa L. Christensen,‡ Christian Jacobsen,§ Søren K. Moestrup,§ Michael Etzerodt,‡ and Hans C. Thøgersen*,‡

Laboratory of Gene Expression, Department of Molecular and Structural Biology, and Department of Medical Biochemistry, University of Aarhus, Aarhus, Denmark

Received March 3, 2000; Revised Manuscript Received May 18, 2000

ABSTRACT: The low-density lipoprotein receptor-related protein (LRP) is a large surface receptor that mediates binding and internalization of a large number of structurally and functionally unrelated ligands. The ligand binding sites are located in clusters of complement-type repeats (CR), where the general absence of mutual binding competition suggests that different ligands map to distinct sites. Binding of α_2-macroglobulin−protease complexes to the LRP is mediated by the receptor binding domain (RBD) of α_2-macroglobulin (α_2M). To determine the major binding epitope(s) in the LRP, we generated a complete set of tandem CR proteins spanning the second cluster of CR domains, and identified a binding site for α_2M in the N-terminal part of the cluster comprising CR3−CR6, using ligand blotting and surface plasmon resonance (SPR) analysis. The specific site involved in α_2M recognition resides in the fourth CR domain, CR4, whereas another site is identified in CR5. An acidic epitope in CR4 is identified as important for binding α_2M by mutagenesis and SPR analysis. The formation of the complex between the rat α_1-macroglobulin RBD and CR domain pairs is characterized by analytical size-exclusion chromatography, which demonstrates a sufficiently strong interaction between the α_1M RBD and CR34 or CR45 for the isolation of a complex.

Human α_2-macroglobulin (α_2M)[1] is a tetrameric protease inhibitor composed of four identical 180 kDa subunits, capable of inhibiting proteases of all known classes (reviewed in ref *1*). The native state of α_2M contains a surface-exposed peptide (the "bait region") representing a recognition site for multiple proteases. Upon cleavage of the bait region, α_2M undergoes a large conformational change leading to activation of an internal γ-glutamyl-β-cysteinyl thiolester bond. The thiolester moiety is hereafter able to attack lysine residues in the protease, leading to covalent attachment of the protease to α_2M. As a consequence of the structural transformation of α_2M upon formation of the complex with the protease, the C-terminal receptor binding domain (RBD) of each subunit becomes exposed (*2*), and the α_2M−protease complex may then be endocytosed via the α_2M receptor pathway (*3*, *4*). Reaction of the thiolester moiety with small nucleophiles, such as methylamine, induces a similar conformational change in α_2M, and results in the generation of transformed α_2M (α_2M*). The RBD of rat α_1-macroglobulin (α_1M) (residues 1319−1474) is also able to bind the receptor, with the same high affinity as the entire light chain from α_1M (*5*). The structure of the RBD from α_2M has been determined (*6*, *7*), and residues found by site-directed mutagenesis studies to be important for receptor binding (*8*, *9*) identify a unique surface-displayed α-helix as being important for receptor binding.

The low-density lipoprotein receptor-related protein (LRP) was cloned and found to be structurally and biochemically similar to the low-density lipoprotein receptor (LDLR) (*10*) and subsequently identified as the α_2M receptor (*3*, *4*). The LRP is multifunctional and serves a role in clearing a wide range of diverse macromolecular ligands from circulation. Besides α_2M−protease complexes, various lipoproteins and lipoprotein-containing particles (*11*), proteases complexed with various serpins, and unrelated proteins such as malaria circumsporozoite protein (*12*), minor group human rhinovirus (*13*), and the β-amyloid precursor protein (APP) (*14*) may be internalized via the LRP. The physiological importance of the LRP is further underscored by studies suggesting that

† This work was supported by Grant 9901730 from the Danish National Science Research Council.

* To whom correspondence should be addressed. E-mail: hct@biobase.dk. Fax: +45 86 18 01 85. Telephone: +45 86 20 20 00.

‡ Department of Molecular and Structural Biology.

§ Department of Medical Biochemistry.

[1] Abbreviations: LRP, low-density lipoprotein receptor-related protein; CR, complement-type repeat from LRP; RAP, receptor-associated protein; α_2M, α_2-macroglobulin (human); α_2M*, methylamine-activated α_2M; α_1M, α_1-macroglobulin (rat); RBD, receptor binding domain; LDLR, low-density lipoprotein receptor; EGF, epidermal growth factor; APP, β-amyloid precursor protein; SPR, surface plasmon resonance; LB, ligand binding repeat from LDLR; PAGE, polyacrylamide gel electrophoresis; U-CR*xy*, fusion protein containing ubiquitin and CR domains *x* and *y*; TFPI, tissue factor pathway inhibitor.

10.1021/bi000498h CCC: $19.00
Published on Web 08/08/2000

the LRP and several of its ligands, in particular, apolipoprotein E (*15*) and APP (*14*), are involved in brain-specific cellular processes that affect the onset of Alzheimer's disease.

The processing of the LRP requires the presence of the receptor-associated protein (RAP) (*16*), a folding chaperone that is a universal antagonist for all other ligand binding to the LRP (*17*).

The members of the receptor family, the LDLR-like receptors, are all mosaic proteins assembled from a variety of protein modules, including two classes of cysteine-rich small domains: the epidermal growth factor (EGF) repeat and the complement-type repeat (CR), also known as the ligand-binding (LB) or class A repeat. Other characteristic components are regions with a 6-fold YWTD consensus sequence proposed to form a compact β-propeller domain (*18*), a single transmembrane helix, and a cytoplasmic tail containing common internalization signal(s), the NPXY motif. The CR domains consist of ~40 amino acids, containing three conserved disulfide bridges and acidic residues forming a conserved calcium cage in each domain (*19*, *20*). Ligand binding to LDLR-like receptors has been shown to involve binding to the CR repeats, which are grouped in clusters with various multiplicities. The 31 CR repeats in the LRP occur in groups of 2 (cluster I), 8 (cluster II), 10 (cluster III), and 11 (cluster IV), counting from the N-terminal end (reviewed in ref *21*). The structures of the third (CR3) and eighth (CR8) domains have recently been elucidated (*22*, *23*).

The interaction between the LRP and α_2M* can be competed by tissue factor pathway inhibitor (TFPI) (*24*) as well as by RAP, suggesting that their binding sites on LRP overlap partially.

The binding of α_2M* to the LRP has previously been mapped to a CNBr-generated fragment comprising cluster II flanked by one N-terminal and two C-terminal EGF repeats (*25*). Subsequent studies confirmed the binding of α_2M* to cluster II, and further suggested that the binding site is located in the N-terminal region of this cluster (*26*, *27*). The preceding EGF repeat has been suggested to contain an epitope for binding of α_2M (*28*), and recently, CR3 was reported to interact weakly ($K_d \sim 140$ μM) with the human α_2M RBD (*22*). The study presented here was undertaken to characterize in detail the binding sites in cluster II for α-macroglobulins, and evidence is provided here for a specific binding involving an acidic epitope in CR4.

EXPERIMENTAL PROCEDURES

Construction of the Expression Plasmid, Site-Directed Mutagenesis, and Protein Production. Expression, purification, and factor Xa processing of U-CR34, -45, -56, -67, -78, -89, and -910 have been described previously (*29*). The expression plasmid (pT7H6UbiFXEGFCR34) for U-EGFCR34 (LRP residues G803−R934) was constructed in a manner similar to that of the expression plasmids described earlier (*29*), with the following set of primers: 5′-GGC GGA TCC ATC GAG GGT AGG GGC ACC AAC AAA TGC CGG-3′ and 5′-GGC AAG CTT AGC GGG CTG AAC AAG TG-3′. Expression of U-EGFCR34 was essential as for U-CR*xy* using RAP affinity purification (*29*).

The rat α_1M RBD was expressed and refolded as described previously (*5*), and methylamine-activated human α_2M was a kind gift from L. Sottrup-Jensen (University of Aarhus).

Mutations were generated using the Quickchange kit (Stratagene, La Jolla, CA) and pT7H6UbiFXCR34 (*29*) as a template for mutagenesis. Mutagenesis primers were from DNA Technology A/S (Aarhus, Denmark). The initial melting temperature of all primers used for mutagenesis was designed to be at least 62 °C, and mutation sites were located in the central region of the primers. All constructs were verified by DNA sequencing using the Thermo Sequenase II dye terminater cycle sequencing kit (Amersham Pharmacia Biotech Inc.).

[^{125}I]α_2M Ligand Blotting.* Radiolabeling of α_2M* was carried out as previously described (*30*). Polyacrylamide gels (18%) were stained with Coomassie Brilliant Blue, or the contents were electroblotted onto nitrocellulose membranes using a semidry electroblotting system (Kem-En-Tec A/S, Copenhagen, Denmark). Membranes were blocked for 15 min with 100 mM Tris-HCl (pH 8.0), 0.9% NaCl, and 2% Tween-20, washed twice for 15 min with MB+BSA [10 mM HEPES (pH 7.4), 2 mM $CaCl_2$, 1 mM $MgCl_2$, 140 mM NaCl, and 2% bovine serum albumin], incubated for 16 h at 4 °C with 5 mL of ^{125}I-labeled α_2M* (10^6 cpm/mL), and finally washed three times for 15 min with MB+BSA. Autoradiography was performed using a PhosphorImager system (Molecular Dynamics, Sunnyvale, CA).

Surface Plasmon Resonance (SPR) Analysis. α_2M* was immobilized on a CM5 BIAcore sensor chip using the Amine Coupling Kit as described by the manufacturer (BIAcore). After chip activation by the injection of 0.2 M *N*-ethyl-*N*-[3-(dimethylamino)propyl]carbodiimide and 0.05 M *N*-hydroxysuccinimide, purified and methylamine-activated α_2M was diluted to a concentration of 80 μg/mL by addition of 10 mM sodium acetate (pH 5.0) and passed through the BIAcore flow cell at a flow rate of 5 μL/min. After protein coupling, the BIAcore chip was capped by exposure to 1 M ethanolamine (pH 8.5). The total protein coupling yield was 41 fmol/mm^2. Protein binding analysis was performed at a flow rate of 5 μL/min with analyte proteins in 10 mM HEPES (pH 7.4), 150 mM NaCl, 5 mM $CaCl_2$, 1 mM EGTA, and 0.05% Tween 20 (Ca-HBS). Before the protein sample was loaded, the chip was equilibrated in Ca-HBS buffer, which also was used as the running buffer. Aliquots of 40 μL of protein samples were injected using the KINJECT option, and regeneration of the sensor chip was performed using 10 mM glycine-HCl (pH 6.0), 500 mM NaCl, and 20 mM EDTA.

Size-Exclusion Analysis. All protein samples were in MB buffer [10 mM HEPES (pH 7.4), 2 mM $CaCl_2$, 1 mM $MgCl_2$, and 140 mM NaCl], and a flow rate of 0.5 mL/min was maintained throughout the analysis. An HR 10/30 Superdex75 (Prep grade) column (Amersham Pharmacia Biotech Inc.) was equilibrated with 2 column volumes of buffer before protein samples of 150 μL were loaded manually using an FPLC system (Amersham Pharmacia Biotech Inc.). Protein samples were either pure CR*xy* (3.5 nmol) or 1:1 mixtures, preincubated for 5 min before loading, of CR*xy* and the rat α_1M RBD (3.5 nmol of each). The absorbance of the effluent at 280 nm was recorded.

Comparative Protein Modeling. Automated comparative protein modeling was performed at the SWISS-MODEL server (http://www.expasy.ch/swissmod/SWISS-MODEL.-html) (*31*, *32*). The CR4 domain was modeled using the First Approach mode of SWISS-MODEL, which provides fully

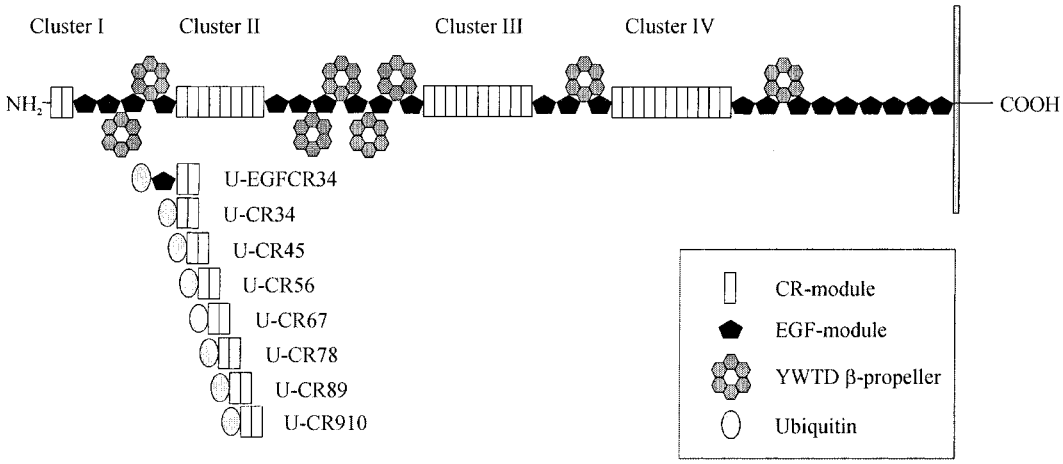

FIGURE 1: Schematic representation of the LRP and the molecular dissection of the second cluster of complement-type repeats. The N-terminal flanking EGF repeat and the eight CR repeats from cluster II were expressed as ubiquitin-fused proteins in *Escherichia coli* as overlapping two-module fragments.

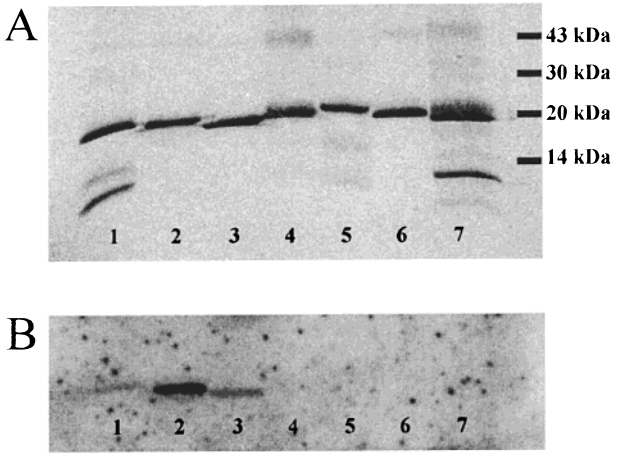

FIGURE 2: [^{125}I]α_2M* blotting of two-repeat fragments of LRP cluster II. (A) Nonreducing SDS−PAGE analysis of equal amounts of the U-CR34, -45, -56, -67, -78, -89, and -910 derivatives (lanes 1−7). (B) Samples identical to those shown in panel A were tested for ligand blotting with [^{125}I]α_2M*, demonstrating a significant interaction with U-CR45 (lane 2), and less efficient binding to U-CR34 (lane 1) and U-CR56 (lane 3).

automated multiple-sequence alignment prior to model building. The construction was based on the available structures of LB1 (PDB entry 1LDL), LB2 (PRB entry 1LDR), LB5 (PDB entry 1AJJ), CR3 (PDB entry 1D2LA), and CR8 (PDB entry 1CR8A) as templates, and the model generation proceeded to completion without human intervention.

RESULTS

Verification of α_2M Affinity for LRP Cluster II.* Figure 1 outlines the structural architecture of the LRP and the dissection of the second ligand binding cluster of CRs into double-repeat receptor fragments produced in *Escherichia coli* as ubiquitin fusion proteins.

We have recently demonstrated efficient binding of RAP to two-repeat fragments of LRP cluster II, and have now also extended this analysis to the mapping of binding sites for α-macroglobulins. Ligand blotting with ^{125}I-labeled human α_2M* to U-CR34, -45, -56, -67, -78, -89, and -910 is shown in Figure 2. Binding of [^{125}I]α_2M* was observed for U-CR34, U-CR45, and U-CR56, with U-CR45 exhibiting the strongest binding.

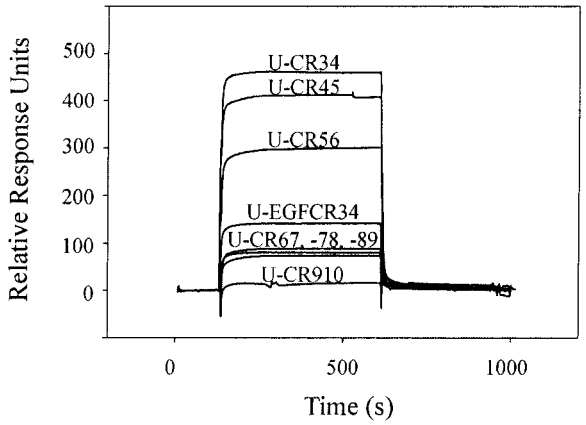

FIGURE 3: SPR analysis of the binding of overlapping two-repeat proteins to α_2M*. Sensorgrams from analysis of U-CR*xy* binding to immobilized α_2M* are shown for 10 μM U-CR34, -45, -56, -67, -78, -89, and -910, as indicated for each sensorgram.

U-CR34 to -89 derivatives immobilized on biosensor chips were used previously for studying the binding of RAP and RAP domains (*29*). However, equivalent studies with α_2M* were not conclusive, probably due to the size of α_2M (720 kDa). Similar problems have previously been encountered in other SPR studies using α_2M* (S. K. Moestrup, personal communication). Accordingly, we immobilized α_2M*, and tested the binding of receptor fragments over a range of concentrations. Figure 3 shows the binding of 10 μM U-CR*xy*. Both U-CR34 and U-CR45 bound strongly to α_2M*, and weaker binding of U-CR56 was also detected. No binding was found for U-CR67, -78, -89, and -910.

The apparent dissociation constants for the binding between α_2M* and U-CR34, -45, and -56 were estimated by fitting the sensorgrams in Figure 3 using a simple 1:1 Langmuir binding model (BIAevaluation 3.0, BIAcore) to be ~20, ~20, and ~300 μM, respectively.

Because binding of α_2M* to the LRP has been proposed to depend on the N-terminal flanking EGF repeat, we tested if the EGF repeat could enhance the affinity for α_2M*. We extended the U-CR34 expression plasmid to include the EGF repeat, and expressed and purified the U-EGFCR34 protein using RAP affinity chromatography. An almost homogeneous product was obtained as judged by nonreducing SDS−PAGE

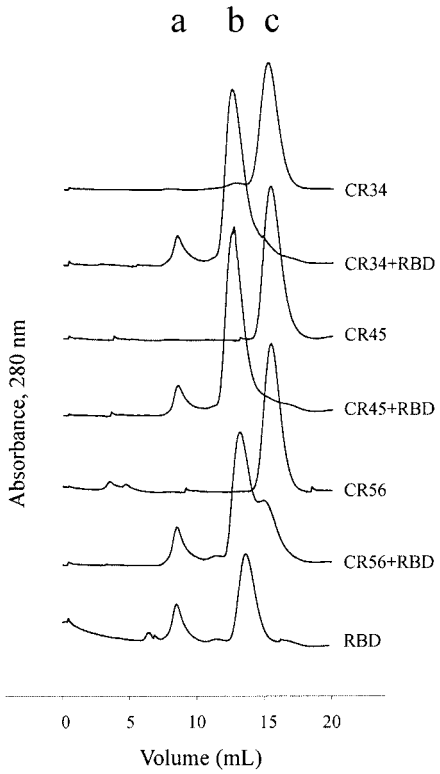

FIGURE 4: Analytical size-exclusion chromatography of the α_1M RBD binding to CR34, CR45, and CR56. Single elution peaks at position c were observed for the two-domain derivatives CR34, CR45, and CR56, as indicated. Preincubation with a molar equivalent of the α_1M RBD to CR34 (CR34+RBD) or CR45 (CR45+RBD) resulted in a shift of the peak toward migration of a stoiciometric complex at position b. Incubation of CR56 with the α_1M RBD (CR56+RBD) resulted in a peak eluting neither at position b nor at the position of the pure RBD. An impurity in the sample of the α_1M RBD (RBD) was used as an internal standard at position a.

analysis. The presence of a small amount of noncorrect folded species suggests that the RAP affinity purification procedure selects only for correctly folded CR modules. Notably, U-EGFCR34 was found to exhibit weaker affinity for the α_2M* biosensor chip than U-CR34 (Figure 3).

Specific Binding and/or Isolation of the Complex between the α_1M RBD and CR34 or CR45. To further confirm the specific binding of α-macroglobulins, we tested the binding of the α_1M RBD to the receptor fragments by analytical size-exclusion chromatography. After liberation of the ubiquitin fusion partner from U-CR*xy* by specific proteolytic cleavage, the two-repeat proteins (CR*xy*) were subjected to analytical gel filtration on Superdex75, with or without the α_1M RBD added in a 1:1 molar ratio. Pure CR34 and CR45 produced elution profiles with peak positions relative to total column volume (V_e/V_c) at 0.66 (~15.5 mL) and the pure α_1M RBD at 0.58 (~13.5 mL) (Figure 4). A single higher peak was eluted at 0.53 (~12.5 mL) when either CR34 or CR45 was preincubated with the α_1M RBD in a 1:1 stoichiometry. The occurrence of only one single new peak, and the fact that there was no detectable peak corresponding to either monomeric protein, suggested the formation of a 1:1 complex. Similar experiments with other two-repeat proteins, e.g., CR56, did not produce single peaks corresponding to unique stable complexes, but resulted only in partial shifting toward the elution position for the stable complexes. This suggested a crucial importance of CR4 for high-affinity binding, as this repeat is shared by both CR34 and CR45.

Identification of Acidic Residues in CR4 That Are Important for Binding α_2M.* Because the binding of the RBD to the LRP is dependent on lysine residues, we decided to test the acidic residues in CR4 for their possible involvement in binding to α_2M*. As seen from an alignment of the sequences of the eight CR modules of LRP cluster II (Figure 5), the four acidic residues, which are proposed to coordinate calcium via their side chains, are strictly conserved. CR4 contains a total of eight acidic residues, and we therefore substituted Asn for Asp and Gln for Glu at positions 898 (D → N), 903 (E → Q), 917 (D → N), and 924 (E → Q), which are not involved in calcium binding, by site-directed mutagenesis.

Mutant U-CR34D917N was previously shown to bind calcium efficiently, suggesting correct folding of this protein (*29*). The three remaining mutant derivatives could be purified using RAP affinity chromatography, indicating correct folding of these three proteins as well. The binding of U-CR34 mutant derivatives to α_2M* was studied by SPR analysis, and the effect of removing the negative charge may be deduced from the sensorgrams shown in Figure 6. U-CR34D898N bound almost as efficiently as wild-type U-CR34, whereas U-CR34E903Q, U-CR34D917N, and U-CR34E924Q all exhibited a substantially reduced level of binding to α_2M*.

Mutation of residue 917 (D → N) virtually eliminated binding to α_2M*. Therefore, the effects of D → N mutation of the corresponding residues in CR3 (D876) and CR5 (D958) were also investigated. A data summary is given in Table 1. U-CR34D876N and U-CR45D958N were both previously verified as correctly folded by calcium binding analysis (*29*).

Currently, three-dimensional structures of five CR domains [LB1 (*33*), LB2 (*34*), LB5 (*19*), CR3 (*22*), and CR8 (*23*)] are known. Their levels of sequence conservation (residue identity) with respect to the sequence of CR4 are 41, 55, 41, 54, and 50%, respectively, and they were therefore found to be suitable as templates for constructing a three-dimensional model of CR4 using the SWISS-MODEL facilities. The coordinates of the model were built using ProModII (*32*), and model refinement was performed by energy minimization using the force field Gromos96 (*35*). The resulting model is shown in Figure 7. Because of the high level of sequence similarity with the templates, alignment with CR4 appeared to be successful, and modeling resulted in the generation of a CR4 model that did not exhibit any obvious discrepancies as judged from the similar fold of the putative CR4 structure compared to the fold of CR3 and CR8 (Figure 7A) and LB1, LB2, and LB5 (not shown).

In the putative structure of CR4, the side chains of the four residues (D898, E903, D917, and E924) are located on the surface of the module, as expected for residues that may be involved in interaction with the RBD domain. The aspartic acid side chains of D876 and D1085 (in CR3 and CR8, respectively), corresponding to D917 in CR4, are located on the surface of these domains, as inferred from their determined structures (*22, 23*), while their backbone carbonyl oxygens are in positions available for calcium coordination. Interestingly, E903 and E924 are surface-located with a distance of ~6.5 Å, which is comparable with the distance

```
                                                    ⇓  ↓ ⇓ ↓      ↓↓
CR3, 849-890    .....VPPPQ CQ.PGEFACA N..SRCIQER WKCDGDNDCL DNSDEAPALC
CR4, 891-931    ......HQHT CP.SDRFKCE N..NRCIPNR WLCDGDNDCG NSEDESNATC
CR5, 932-971    ......SART CP.PNQFSCA S..GRCIPIS WTCDLDDDCG DRSDES.ASC
CR6, 972-1011   ......AYPT CFPLTQFTCN N..GRCININ WRCDNDNDCG DNSDE..AGC
CR7, 1012-1051  .......SHS CS.STQFKCN S..GRCIPEH WTCDGDNDCG DYSDETHANC
CR8, 1052-1097  TNQATRPPGG CH.TDEFQCR L.DGLCIPLR WRCDGDTDCM DSSDE..KSC
CR9, 1098-1140  ....EGVTHV CDPSVKFGCK D.SARCISKA WVCDGDNDCE DNSDE..ENC
CR10, 1141-1182 ......ESLA CR.PPSHPCA NNTSVCLPPD KLCDGNDDCG DGSDEG.ELC
```

FIGURE 5: Primary structures of complement-type repeats from cluster II of the LRP. An alignment of the sequences of CR3−CR10 is shown in register with the six strictly conserved cysteine residues. Residues coordinating calcium via their side chain are marked with ↓ and via their backbone carbonyl with an open down arrow. The four acidic residues of CR4, which are mutated in our binding analysis and proposed to be important for binding to α_2M*, are highlighted.

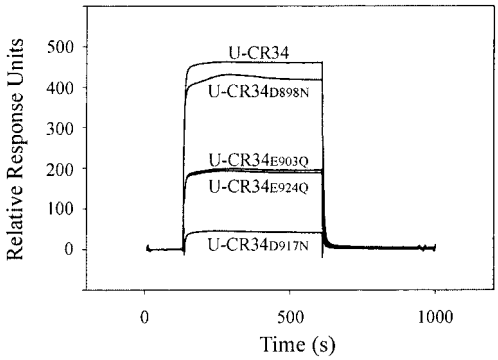

FIGURE 6: SPR analysis of CR4 mutants (D → N and E → Q) binding to α_2M*. Sensorgrams for analysis of U-CR34 single-residue mutant derivatives at 10 μM in binding to immobilized α_2M* are shown, as indicated for each sensorgram.

Table 1: U-CR*xy* Derivatives Binding to α_2M*

U-CR*xy*	plateau response units[a]	U-CR*xy*	plateau response units[a]
U-CR34 wt	460 RU	U-CR34E924Q	188 RU
U-CR34D876N	205 RU	U-CR45 wt	407 RU
U-CR34D898N	418 RU	U-CR45D917N	46 RU
U-CR34E903Q	194 RU	U-CR45D958N	49 RU
U-CR34D917N	42 RU		

[a] Representative plateau response levels (values at 550 s) for 10 μM U-CR*xy* derivatives. The values are given as single measurements, but the results have been confirmed with different flow cells with varying amounts of immobilized α_2M* and with other concentrations of U-CR*xy* showing similar results. The values are therefore not expected to deviate more than ±10%.

between the two essential lysine residues identified in the α_2M RBD (*6*, *8*).

DISCUSSION

The study presented here proposes the existence of an epitope in LRP cluster II, important for recognition of α-macroglobulins. On the basis of [^{125}I]α_2M* ligand blotting and SPR binding analysis of overlapping two-repeat receptor fragments, the major binding site was located on CR4. This result was confirmed using the α_1M RBD to study the complex formation with CR domain pairs by analytical size-exclusion chromatography.

On the basis of previous reports showing that the binding of α-macroglobulins is dependent on lysine residues, we examined the effect of eliminating the negative charges of all acidic residues not involved in Ca^{2+} coordination. Two unique glutamic acid residues, Glu903^{CR4} and Glu924^{CR4} in the sequence of CR4, were identified by SPR analysis as being equally important for the specific binding between

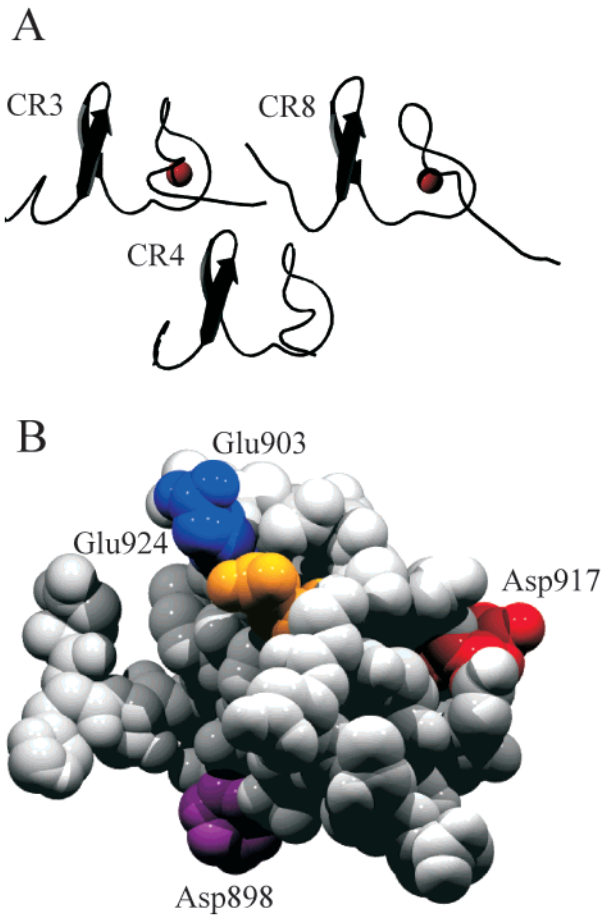

FIGURE 7: Modeling of the CR4 structure. (A) Ribbon diagrams comparing the similar folds of CR3 and CR8 with the modeled structure of CR4. The calcium ion is shown as a red sphere for CR3 and CR8. (B) Putative structure of CR4, showing the location of the four CR4 mutants, used in the α_2M* SPR binding analysis (Figure 6). The color code is as follows: Asp898, violet; Glu903, blue; Asp917, red; and Glu924, yellow. The model was generated using automated comparative modeling at the SWISS-MODEL server, and the figure was prepared with the Swiss-Pdb Viewer (*38*) and rendered with POV-Ray (http://www.povray.org).

U-CR34 and α_2M*. In the structural model of CR4, these two residues are predicted to be located at the surface of CR4, with a distance of ∼6.5 Å. The two essential positively charged residues in the RBD, Lys1370$^{\alpha_2M}$ and Lys1374$^{\alpha_2M}$, noted to be important for the efficient LRP binding (*8*, *9*), are located on a surface-displayed α-helix (*6*, *36*), also with a distance of ∼6.5 Å. It is therefore tempting to speculate that LRP interacts with α_2M* specifically via a significant contribution from the negative Glu epitope in LRP^{CR4} and the positive Lys epitope in the α_2M RBD.

D917 was shown to be important for proper recognition of RAP (*29*) and other LRP ligands (O. M. Andersen, unpublished experiments). The effect of mutation of residue 917 (D → N) in this study showed that D917 is also important for recognition of α_2M*. The effect of mutation of aspartic acid residue 917 in U-CR34 was further examined by studying the effect of the same mutation in U-CR45 (U-CR45D917N), and these studies confirmed that D917 is critical for α_2M* binding. Analysis of mutants in which the corresponding conserved aspartic acid residue in CR3 (U-CR34D876N) or CR5 (U-CR45D958N) was altered also exhibited a decreased affinity for α_2M*.

These results indicate that binding of α-macroglobulin involves multiple CR domains, in agreement with other reports suggesting that high-affinity binding requires multiple contributions. The preference for CR4 binding reported here provides a substantial contribution not only to overall affinity but also possibly significantly to the specificity of the interaction. Another binding site located in CR5, as indicated by the low-affinity binding between α_2M* and U-CR56, contributes further to the high affinity.

The apparent dissociation constant for binding between U-CR34 (and U-CR45) and immobilized α_2M* was estimated to be ~20 μM. Dolmer et al. reported a dissociation constant of 140 μM for the binding between CR3 and a truncated form of the human α_2M RBD in solution (*22*). The use of immobilized α_2M* in this study is likely to represent a similar surface of RBD as if RBD itself has been immobilized, thereby sugggesting that a direct comparison can be justified. Therefore, it seems likely that the binding between a single RBD and a small receptor fragment contributes to the overall affinity with a dissociation constant in the micromolar range. The apparent affinity (~2 nM) of α_2M−protease complexes for the LRP is much higher due to simultaneous binding of several subunits of α_2M to several LRPs and several binding sites in the LRP (*30*).

The hypothesis of multiple binding sites is further substantiated as the second and fourth clusters of CR modules of LRP were shown to bind common ligands, e.g., α_2M*, tissue-type plasminogen activator−plasminogen activator inhibitor 1 complexes, apolipoprotein E, TFPI, and lactoferrin (*37*). Comparison of the sequences of these two clusters shows the presence of a glutamic acid residue corresponding to $Glu924^{CR4}$ in CR23, located in cluster IV.

Contrary to previous suggestions, the N-terminal flanking EGF repeat was found not to enhance the affinity for α_2M*. Recently, Neels et al. reported α_2M* binding of a fragment spanning EGFCR3−CR7, but were unable to detect any binding to a fragment comprising EGFCR34 (*37*). This was unexpected, but in accord with our own observation of a decreased α_2M* affinity for U-EGFCR34 compared to that for U-CR34. However, the more efficient binding of α_2M* upon inclusion of CR5−CR7 is in agreement with the identification of a minor binding site for α_2M* in CR5.

This paper presents the first identification of a specific interaction site for ligand binding to the LRP. The ability to isolate a ligand−receptor fragment complex offers a unique starting point for structural studies that may provide specific clues to explain how the ability of the LRP to recognize its broad spectrum of dissimiliar ligands is encoded in an array of similar ligand binding domains.

ACKNOWLEDGMENT

We thank Anne Marie Bundsgaard and Ove Lillelund for technical assistance and Dr. J. Herz for providing human LRP cDNA.

REFERENCES

1. Sottrup-Jensen, L. (1989) *J. Biol. Chem. 264*, 11539−11542.
2. Van Leuven, F., Marynen, P., Sottrup-Jensen, L., Cassiman, J. J., and Van den Berghe, H. (1986) *J. Biol. Chem. 261*, 11369−11373.
3. Strickland, D. K., Ashcom, J. D., Williams, S., Burgess, W. H., Migliorini, M., and Argraves, W. S. (1990) *J. Biol. Chem. 265*, 17401−17404.
4. Kristensen, T., Moestrup, S. K., Gliemann, J., Bendtsen, L., Sand, O., and Sottrup-Jensen, L. (1990) *FEBS Lett. 276*, 151−155.
5. Nielsen, K. L., Sottrup-Jensen, L., Fey, G. H., and Thøgersen, H. C. (1995) *FEBS Lett. 373*, 296−298.
6. Jenner, L., Husted, L., Thirup, S., Sottrup-Jensen, L., and Nyborg, J. (1998) *Structure 6*, 595−604.
7. Huang, W., Dolmer, K., Liao, X., and Gettins, P. G. W. (2000) *J. Biol. Chem. 275*, 1089−1094.
8. Nielsen, K. L., Holtet, T. L., Etzerodt, M., Moestrup, S. K., Gliemann, J., Sottrup-Jensen, L., and Thøgersen, H. C. (1996) *J. Biol. Chem. 271*, 12909−12912.
9. Howard, G. C., Yamaguchi, Y., Misra, U. K., Gawdi, G., Nelsen, A., DeCamp, D. L., and Pizzo, S. V. (1996) *J. Biol. Chem. 271*, 14105−14111.
10. Herz, J., Hamann, U., Rogne, S., Myklebost, O., Gausepohl, H., and Stanley, K. K. (1988) *EMBO J. 7*, 4119−4127.
11. Beisiegel, U., Weber, W., Ihrke, G., Herz, J., and Stanley, K. K. (1989) *Nature 341*, 162−164.
12. Shakibaei, M., and Frevert, U. (1996) *J. Exp. Med. 184*, 1699−1711.
13. Hofer, F., Gruenberger, M., Kowalski, H., Machat, H., Huettinger, M., Kuechler, E., and Blass, D. (1994) *Proc. Natl. Acad. Sci. U.S.A. 91*, 1839−1842.
14. Kounnas, M. Z., Moir, R. D., Rebeck, G. W., Bush, A. I., Argraves, W. S., Tanzi, R. E., Hyman, B. T., and Strickland, D. K. (1995) *Cell 82*, 331−340.
15. Schmechel, D. E., Saunders, A. M., Strittmatter, W. J., Crain, B. J., Hulette, C. M., Joo, S. H., Pericak-Vance, M. A., Goldgaber, D., and Roses, A. D. (1993) *Proc. Natl. Acad. Sci. U.S.A. 90*, 9649−9653.
16. Bu, G., and Rennke, S. (1996) *J. Biol. Chem. 271*, 22218−22224.
17. Strickland, D. K., Ashcom, J. D., Williams, S., Battey, F., Behre, E., McTigue, K., Battey, J. F., and Argraves, W. S. (1991) *J. Biol. Chem. 266*, 13364−13369.
18. Springer, T. A. (1998) *J. Mol. Biol. 283*, 837−862.
19. Fass, D., Blacklow, S., Kim, P. S., and Berger, J. M. (1997) *Nature 388*, 691−693.
20. Brown, M. S., Herz, J., and Goldstein, J. L. (1997) *Nature 388*, 629−630.
21. Neels, J. G., Horn, I. R., van den Berg, B. M. M., Pannekoek, H., and van Zonneveld, A.-J. (1998) *Fibrinolysis Proteolysis 12*, 219−240.
22. Dolmer, K., Huang, W., and Gettins, P. G. W. (2000) *J. Biol. Chem. 275*, 3264−3269.
23. Huang, W., Dolmer, K., and Gettins, P. G. W. (1999) *J. Biol. Chem. 274*, 14130−14136.
24. Warshawsky, I., Herz, J., Broze, G. J., Jr., and Schwartz, A. L. (1996) *J. Biol. Chem. 271*, 25873−25879.
25. Moestrup, S. K., Holtet, T. L., Etzerodt, M., Thøgersen, H. C., Nykjær, A., Andreasen, P. A., Rasmussen, H. H., Sottrup-Jensen, L., and Gliemann, J. (1993) *J. Biol. Chem. 268*, 13691−13696.
26. Horn, I. R., Moestrup, S. K., van den Berg, B. M. M., Pannekoek, H., Nielsen, M. S., and van Zonneveld, A.-J. (1995) *J. Biol. Chem. 270*, 11770−11775.

27. Horn, I. R., van den Berg, B. M., van der Meijden, P. Z., Pannekoek, H., and van Zonneveld, A.-J. (1997) *J. Biol. Chem. 272*, 13608−13613.
28. Willnow, T. E., Orth, K., and Herz, J. (1994) *J. Biol. Chem. 269*, 15827−15832.
29. Andersen, O. M., Christensen, L. L., Christensen, P. A., Sørensen, E. S., Jacobsen, C., Moestrup, S. K., Etzerodt, M., and Thøgersen, H. C. (2000) *J. Biol. Chem. 275*, 21017−21024.
30. Moestrup, S. K., and Gliemann, J. (1991) *J. Biol. Chem. 266*, 14011−14017.
31. Peitsch, M. C. (1995) *Bio/Technology 13*, 658−660.
32. Peitsch, M. C. (1996) *Biochem. Soc. Trans. 24*, 274−279.
33. Daly, N. L., Scanlon, M. J., Djordjevic, J. T., Kroon, P. A., and Smith, R. (1995) *Proc. Natl. Acad. Sci. U.S.A. 92*, 6334−6338.
34. Daly, N. L., Djordjevic, J. T., Kroon, P. A., and Smith, R. (1995) *Biochemistry 34*, 14474−14481.
35. Van Gunsteren, W. F., Billeter, S. R., Eising, A. A., Hünenberger, P. H., Krüger, P., Mark, A. E., Scott, W. R. P., and Tironi, I. G. (1996) *Biomolecular Simulation: The GROMOS96 Manual and User Guide*, Vdf Hochschulverlag ETH Zürich, Zürich, Switzerland.
36. Huang, W., Dolmer, K., Liao, X., and Gettins, P. G. W. (1998) *Protein Sci. 7*, 2602−2612.
37. Neels, J. G., van den Berg, B. M. M., Lookene, A., Olivecrona, G., Pannekoek, H., and van Zonneveld, A.-J. (1999) *J. Biol. Chem. 274*, 31305−31311.
38. Guex, N., and Peitsch, M. C. (1997) *Electrophoresis 18*, 2714−2723.

BI000498H